Thermochimica Acta, 144 (1989) 313–328
Elsevier Science Publishers B.V., Amsterdam – Printed in The Netherlands

THE REDUCTION OF MANGANESE NODULES BY HYDROGEN

D.N. DRAKSHAYANI, CHITRA SANKAR and R.M. MALLYA
Indian Institute of Science, Bangalore-560012 (India)
(Received 20 September 1988)

ABSTRACT

Manganese nodules, obtained from the Indian Ocean, were characterized by Mössbauer spectroscopy, X-ray powder diffractometry, infrared spectroscopy and subjected to dynamic and isothermal thermogravimetry in hydrogen atmosphere. The activation energies for the reduction of manganese nodules in hydrogen were calculated from isothermal measurements at different temperatures.

INTRODUCTION

Marine manganese nodules are made up mainly of oxides/hydroxides of manganese and iron and, to a lesser extent, of those of Co, Ni and Cu. They are found most frequently at the sediment–water interface in oceans, although some do exist at depth in marine sediments. The nodules vary in diameter from 1 to 25 cm. The characterization of the nodules by Mössbauer spectroscopy, X-ray diffractometry and other techniques has been comprehensively reviewed by Burns and Burns [1].

Marine manganese nodules are potential sources for the future extraction of Cu, Ni and Co. Consequently, extensive studies have been made on their reactivities, leaching characteristics and related studies. A study of the reduction of polymetallic oceanic nodules for their use as catalysts has been made by Dodet et al. [2], who studied the influence of calcination temperature in the range 200–700 °C under nitrogen, hydrogen and oxygen flows. However, their reactivities with hydrogen have not been investigated.

In the present study, therefore, the reactivity of these nodules in hydrogen atmosphere and the kinetics of reduction of manganese nodules in hydrogen have been investigated in detail.

EXPERIMENTAL

The manganese nodules used in the present work were obtained from the Indian Ocean at a depth of 3000 m. Manganese nodules are made up of

0040-6031/89/$03.50

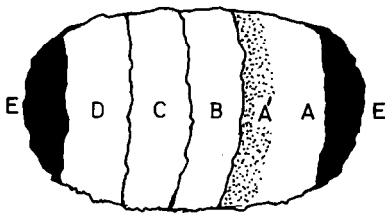

E : BLACK IN COLOUR (SURFACE LAYER)
A : LIGHT YELLOW IN COLOUR
A' : YELLOW WITH BLACK SPOTS
B : WHITE (INNER MOST BAND)
C : BROWNISH BLACK
D : GREY

Fig. 1. A section of the manganese nodule (schematic).

colloform bands; these consist of dark and light bands which are rich in Mn and Fe. Mineralogical studies indicate that it consists of wad (soft, amorphous naturally occurring manganese oxide) and cryptocrystalline goethite.

The manganese nodules were powdered using an agate mortar and pestle and then heated in 100 °C in an oven for 2 h before analysis. The different bands of manganese nodules, A, A′, B, C, D and E, were obtained from a section of the nodule and are shown schematically in Fig. 1. The samples were also heated to 100 °C for 2 h before analysis. The chemical composition of the manganese nodules was determined gravimetrically and volumetrically for major elements such as Fe, Mn and SiO_2 and by atomic absorption spectroscopy for minor elements such as Cu, Co, Ni and other transition metals. A typical analysis of the nodules indicated that they mainly contain the following elements (in wt.%): Mn 17.4, Fe 12.8, Cu 0.34, Co 0.33, Ni 0.62, Cr 0.019, SiO_2 20.13; the percentage weight loss at 100 °C was 4.4. The different bands of the nodules were also analysed for Cu, Co, Ni, Cr and SiO_2. The results are given in Table 1.

The manganese nodules were characterized by X-ray powder diffractometry, Mössbauer spectroscopy (MS), infrared spectroscopy (IR), and their reactivity to hydrogen was investigated using dynamic thermogravimetric (TG) and isothermal studies.

The X-ray diffraction studies were made using Co $K\alpha$ radiation at a scan rate of 2° min^{-1}. The Mössbauer spectra of the various layers of manganese nodules were taken using the constant-acceleration mode. The drive system used was from Wiessel (Germany) and the set-up consisted of multichannel analyser, detector and other components (Canberra Industries Inc., U.S.A.). The detector used was a conventional scintillation detector which consists of NaI(Tl) crystal of 2.54-cm diameter and 1-mm thickness, a photomultiplier

TABLE 1

The chemical analysis of the different layers of manganese nodules

Layer	Element (wt.%) [a]				SiO_2 (%)	Weight loss at 100 °C (%)
	Ni	Cu	Co	Cr		
A	0.316	0.314	0.219	0.008	19.95	0.76
A′	0.111	0.162	0.189		11.76	0.57
B	0.023	0.055	0.058	0.012	28.93	2.99
C	0.128	0.189	0.187	0.011	27.72	1.22
D	0.217	0.281	0.035	0.013	23.67	10.79
E	0.946	0.772	0.163	0.072	5.81	9.12

[a] The balance is Mn, Fe and other trace elements.

tube and voltage divider network. A 25 mCi ^{57}Co source in rhodium matrix was used and all isomer shifts are given with respect to the metallic iron at room temperature. The Mössbauer spectra were computer-fitted using a versatile computer program (MOSFIT) on a DEC 1090 system.

The thermobalance used was a modified version of that developed by Vasudevamurthy et al. [3] using a quartz-fibre spring. The sensitivity of the spring is 19.005 cm g^{-1}. The experimental set-up used for the thermogravimetric studies was similar to that used by Ramani et al. [4]. The hydrogen gas was passed through bubblers containing freshly prepared alkaline pyrogallol and chromous chloride solutions to remove oxygen and then through a $CaCl_2$ tower and over P_2O_5 to remove moisture.

The dynamic TG of sample G and B layer of the manganese nodules was carried out between room temperature and 500 °C in a flowing hydrogen atmosphere with a heating rate of 1 °C min^{-1} and flow rate of 1.8 l h^{-1}. An extensive study was only made for sample G (representative of the nodules); such studies were not made for the other layers because the material available was limited.

RESULTS AND DISCUSSION

X-ray diffraction studies

The X-ray diffractograms of sample G, which is representative of the entire nodule, and portions of different bands are given in Fig. 2. These data indicate the presence of quartz, β-MnO_2, clay minerals, such as kaolinite and phillipsite, and, most probably, an amorphous form of the oxyhydroxide of iron. The outermost band, E, consists of Mn in the form of todorokite and the innermost band, B, consists of β-MnO_2. The middle bands have birnessite and β-MnO_2.

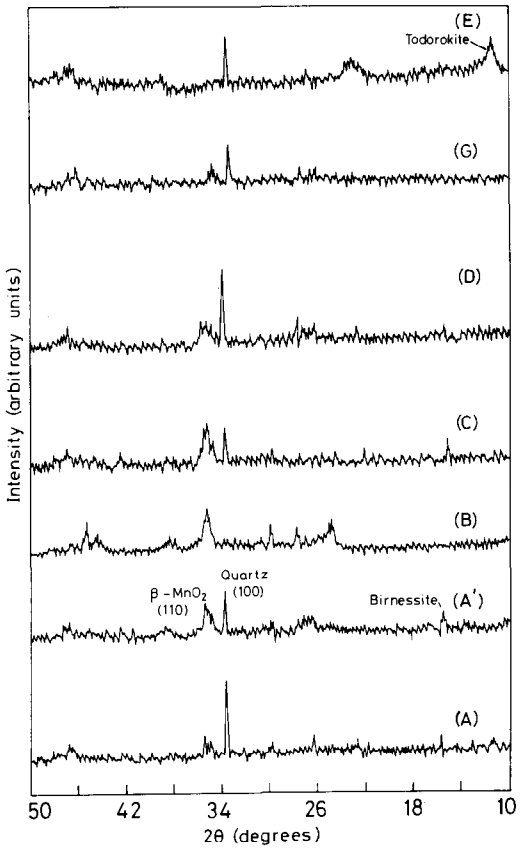

Fig. 2. X-ray diffractograms of G which is representative of the nodule and the different layers of the nodule.

Infrared studies

The IR spectra of G and the various bands (layers) of manganese nodules (Fig. 3) resemble each other and only the intensities of the various bands vary depending on the amount of oxides/hydroxides of Mn, Fe and SiO_2 present. The results are in agreement with the IR spectra obtained by Okada et al. [5] for various oxides and manganese nodules from the Pacific Ocean.

Mössbauer studies

The Mössbauer spectra of the nodules are given in Fig. 4 and the parameters are given in Table 2. The spectra are indicative of Fe in the +3 oxidation state in an octahedral environment of oxygen, OH^- or H_2O.

The X-ray diffraction measurements suggest that, in these manganese deposits, Mn is initially in the form of todorokite and later changes first to birnessite and then to β-MnO_2. Alternatively, it is possible that the various

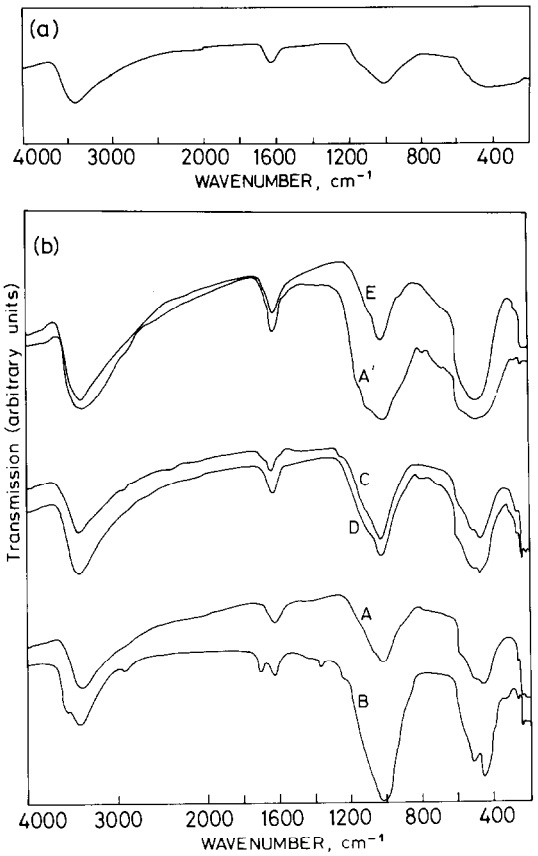

Fig. 3. Infrared spectra of (a) general G, and (b) various layers of the nodule.

TABLE 2

Mössbauer parameters of manganese nodules at room temperature (± 0.041)

Sample	Isomer shift (mm s^{-1})	Quadrupole splitting (mm s^{-1})	Full width at half maximum (mm s^{-1})
General G	0.353	0.662	0.467
Different layers			
A	0.396	0.652	0.458
A′	0.367	0.639	0.427
B	0.357	0.594	0.565
C	0.365	0.620	0.422
D	0.350	0.653	0.537
E	0.367	0.674	0.497

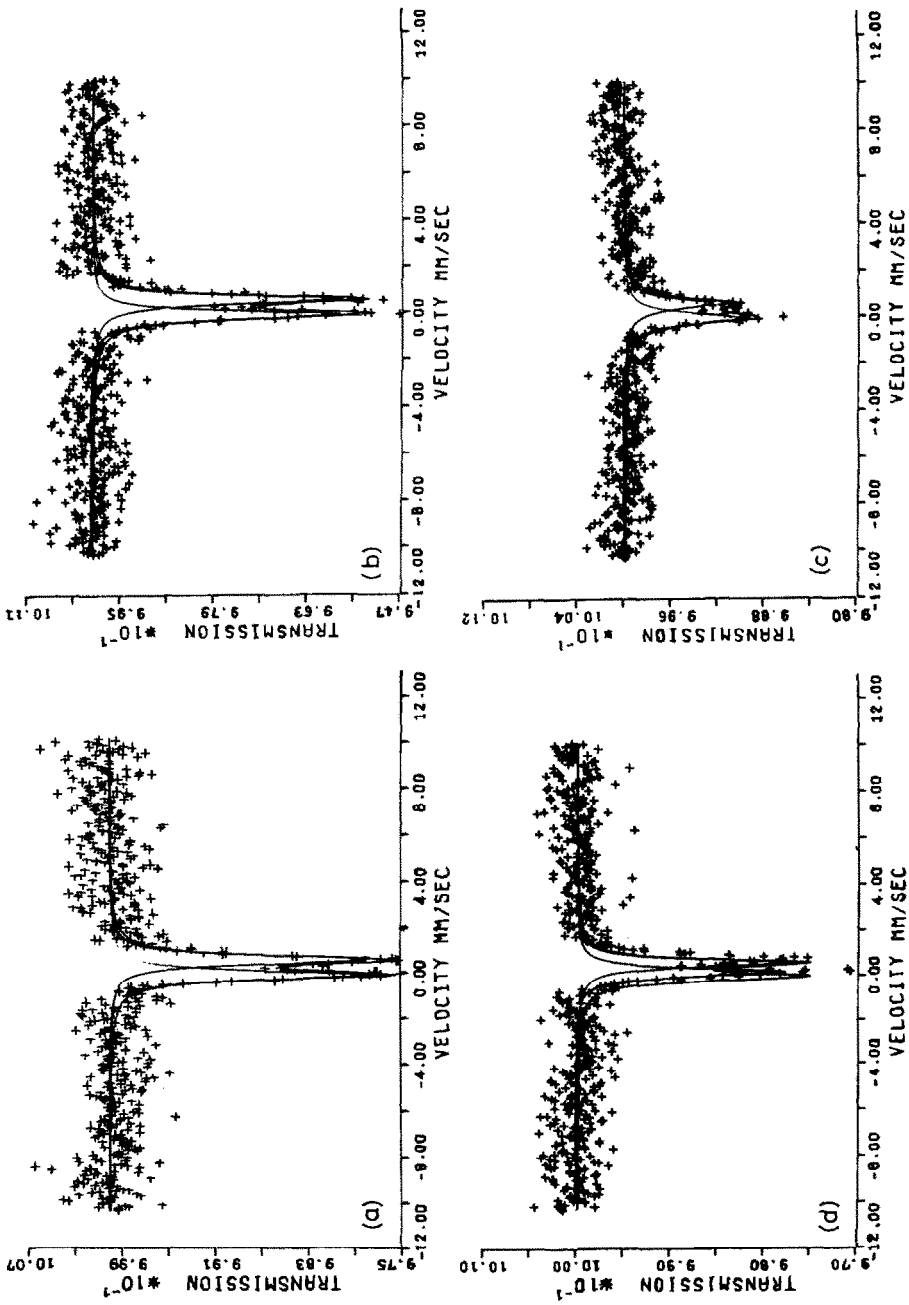

Fig. 4. Mössbauer spectra of (a) general G, (b) layer A', (c) layer B, and (d) layer C.

layers are formed under different conditions. Stevenson and Stevenson [6] have reported the occurrence of birnessite on the outer surfaces of manganese nodules that have dried out during storage in a museum. This suggests that, on long exposure to atmosphere, mineralogical changes may occur in the nodules removed from seawater.

The IR studies indicate that the absorption band at 3400–1400 cm^{-1} is of water or OH^-. The absorption band at 1050–1000 cm^{-1} is due to silicates such as clay minerals and that at 500–400 cm^{-1} is an overlap band of silicate and MnO_2 mineral. The bands at 1050–1000 cm^{-1} and 550–400 cm^{-1} in band B are very strong when compared with other samples; this is because it contains more manganese oxide mineral and SiO_2.

The large widths of the Mössbauer peaks and the range of quadrupole splittings may be explained either by mixtures of different minerals or by variable particle sizes. The higher quadrupole splitting for outer portions than inner portions of nodules can be related to differences in the average size of the particles. This may be due to older (central) parts being formed under different conditions than younger (outer) parts or recrystallization of particles to coarse-grained crystallites occurring inside the manganese nodules in the course of time.

It has been found that Fe^{3+} ions in a variety of oxygen environments have Mössbauer parameters falling in the range observed for manganese nodules. These not only include superparamagnetic or cryptocrystalline goethite, but also clay minerals such as illite or montmorillonite and various hydrated oxyhydroxide polymers or gels. It is therefore not possible to identify unambiguously by Mössbauer spectroscopy the iron bearing minerals in manganese nodules. It can be said that iron is present in the nodules in Fe^{3+} state in an octahedral environment.

Thermogravimetric studies

The TG curves of G and B in H_2 atmosphere are shown in Fig. 5. The TG of G indicates that the reaction proceeds in four stages with a total weight loss of 22% and in the case of B in only two stages with a total weight loss of 8.94%. The percentage which reacted in the two samples at various stages is given in Table 3. The percentage reacted in the B layer is less because it contains mainly manganese oxide mineral and quartz. In both samples the first stage is due to the loss of adsorbed water. This is confirmed by further isothermal studies.

Manganese nodules were reduced isothermally at temperatures of 130, 320, 400, and 500 °C for 1 h and at 400 °C for 8 h in H_2 atmosphere and then cooled to room temperature in H_2 atmosphere. Each of these samples was then characterized by X-ray powder diffractometry, IR spectroscopy and Mössbauer spectroscopy. The X-ray diffractograms and IR spectra are

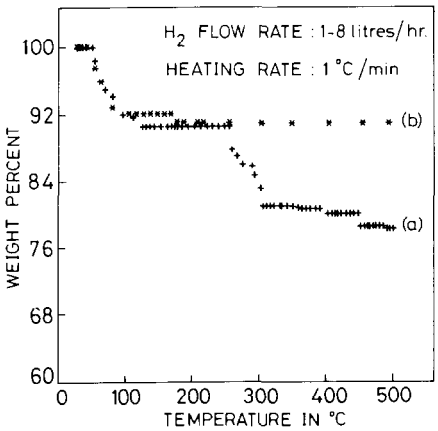

Fig. 5. The TG curves of (a) G reduced in hydrogen, and (b) layer B reduced in hydrogen.

given in Figs. 6 and 7, respectively. The Mössbauer spectra of the reduced samples are given in Fig. 8 and the data in Table 4.

Heating these nodules in hydrogen is expected to give rise to lower iron oxides containing various amounts of other transition-metal impurities which, on further reduction, may give rise to solid solutions or alloys of Fe with other transition-metal ions. The X-ray data of sample G reduced at 130 °C for 1 h and the IR spectrum of the sample indicate that the peak around 3000–3500 cm^{-1} is of lower intensity, which implies that at 130 °C there is no structural change. The Mössbauer spectrum of sample G is similar to that of unreacted G, confirming the above inference. It is concluded, therefore, that the first stage is only due to the loss of adsorbed water or of water from pores.

The X-ray diffractogram of the sample reduced at 320 °C indicates the presence of quartz and manganese oxide minerals. The X-ray diffractograms of the samples reduced at higher temperatures are similar and indicate the presence of quartz. The samples reduced in H_2 may have other transition

TABLE 3

Dynamic TG data of G and B samples

Stages	Sample G		Sample B	
	Temperature range (°C)	Amount reacted (%)	Temperature range (°C)	Amount reacted (%)
I	52–130	8.06	42–117	7.92
II	254–320	13.92	157–176	1.12
III	355–398	4.56		
IV	447–480	0.68		

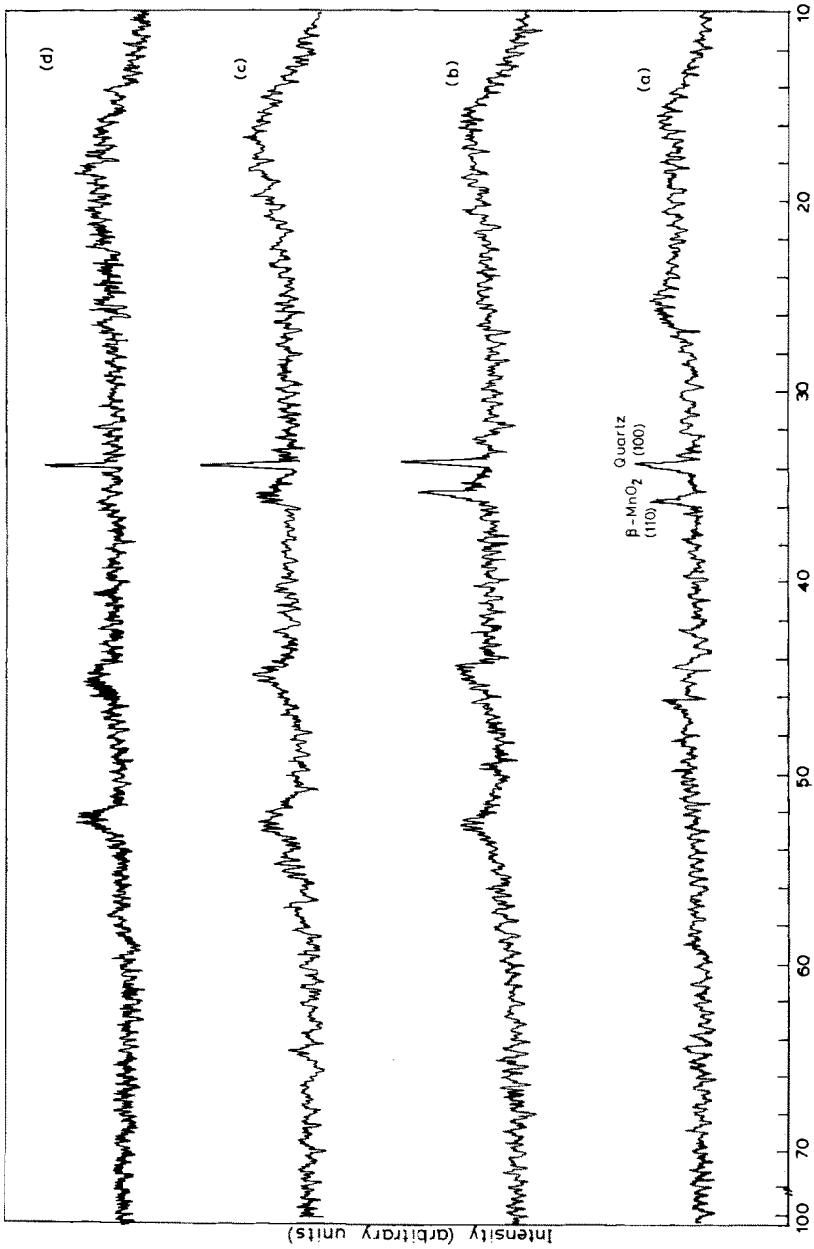

Fig. 6. X-ray diffractograms of manganese nodules isothermally reduced in hydrogen at various temperatures: (a) 130 °C for 1 h, (b) 320 °C for 1 h. (c) 400 °C for 1 h. and (d) 400 °C for 8 h.

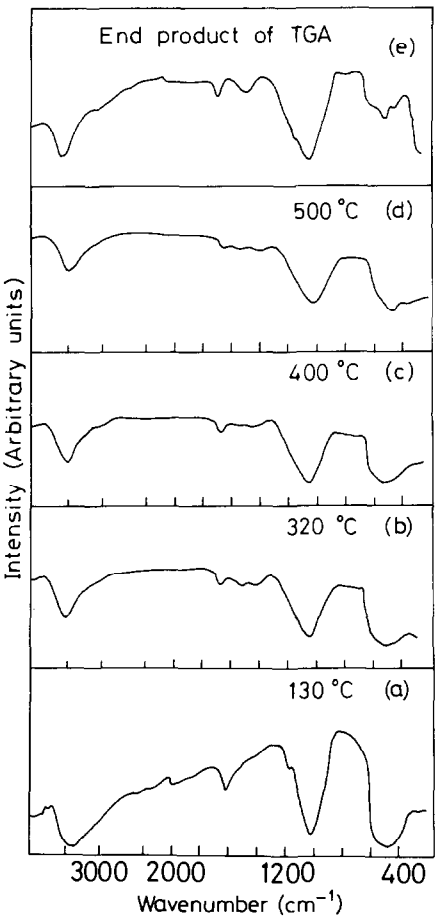

Fig. 7. Infrared spectra of manganese nodules reduced at various temperatures.

elements in metallic form, but in a very finely-divided state and in very low concentrations which are not revealed by X-ray diffractometry. The IR spectra of these samples are similar to that of unreduced G except that the relative intensities vary. The samples reduced at 130 and 320 °C are non-magnetic, whereas the samples reduced at higher temperatures are magnetic. The sample G reduced at 320 °C shows a quadrupole split spectrum and is identical to that exhibited by α-Fe_2O_3 in a superparamagnetic state [7–11]. Ferric oxyhydroxide therefore decomposes to α-Fe_2O_3 in the second stage.

The values of the isomer shift obtained from the Mössbauer spectra of the samples reduced at 400 °C for 1 h and 8 h do not vary with that observed for the reduced sample at 320 °C. However, the spectra exhibit considerable broadening. The sample reduced at 500 °C exhibits an additional quadrupole spectrum and also a hyperfine spectrum corresponding to metallic iron. The third and fourth stages could be due to the reduction of the transition

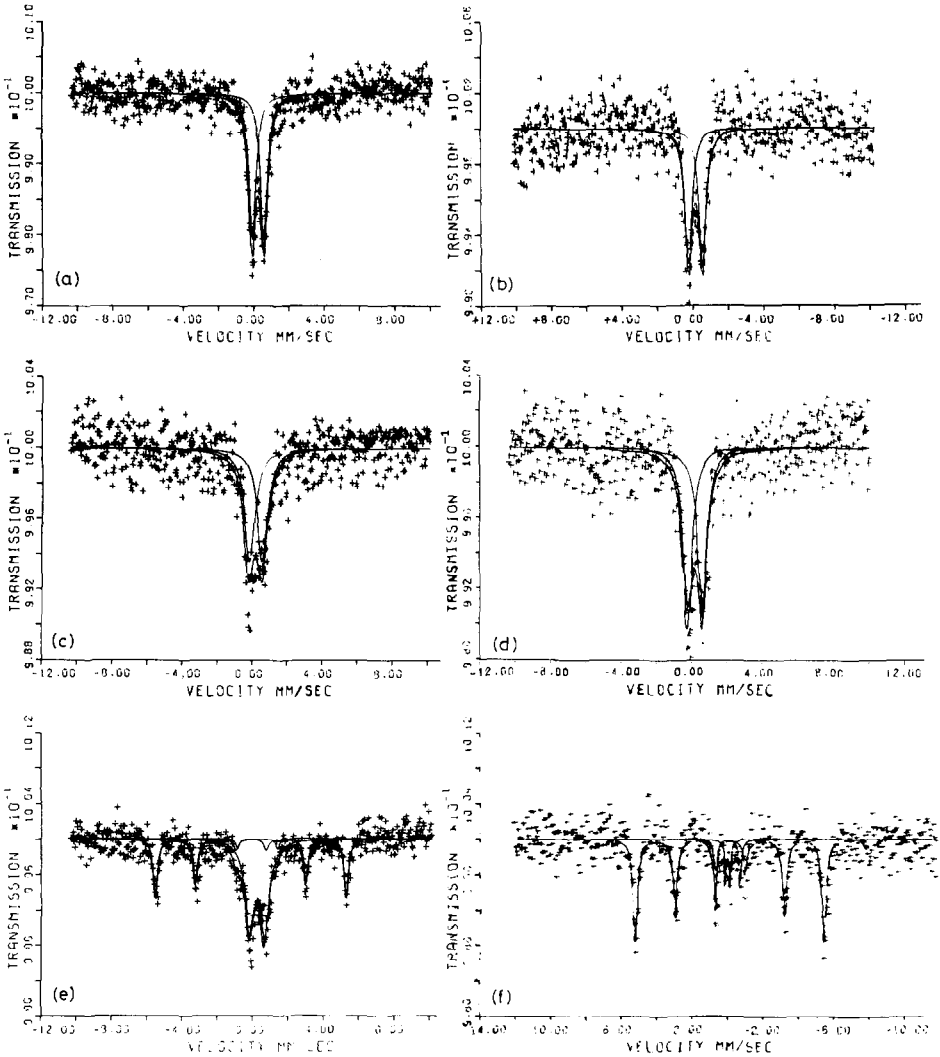

Fig. 8. Mössbauer spectra at room temperature for the nodules reduced at (a) 130 °C for 1 h, (b) 320 °C for 1 h, (c) 400 °C for 1 h, (d) 400 °C for 8 h, (e) 500 °C for 1 h, and (f) the end product of TGA.

metals from their higher oxidation states to lower oxidation states or to the metallic form. The broadening of the original quadrupole spectrum for samples reduced at 400 and 500 °C can be due to the distribution of electric fields around the Fe^{3+} ion due to the presence in its vicinity of Cu, Co and Ni either in lower oxidation states or in solid solution in alloys. It is also noted from Table 4 that the full widths for the samples reduced at 400 °C for 8 h and 500 °C for 1 h are marginally less, indicating a more uniform distribution of electric fields. The second quadrupole present for the latter sample is indicative of Fe^{3+} in the presence of a large electric-field gradient,

TABLE 4

Mössbauer parameters for sample G at room temperature for samples treated in hydrogen atmosphere at various temperatures

Treatment	Isomer shift [a] (mm s^{-1}) ($\pm$0.041)	Quadrupole splitting (mm s^{-1}) (0.041)	Full width at half maximum (mm s^{-1}) ($\pm$0.041)	Internal field (KG) ($\pm$3)	Relative amount of Fe present in different states
130 °C for 1 h	0.371	0.681	0.496		
320 °C for 1 h	0.316	0.772	0.469		
400 °C for 1 h	0.315	0.774	0.732		
400 °C for 8 h	0.313	0.848	0.646		
500 °C for 1 h	0.34	0.854	0.626		0.59
	0.403	2.257	0.226		0.03
			0.306	330	0.38
End product of TG	0.104	0.277	0.149		0.10
	0.125	1.384	0.197		0.08
			0.304	331	0.82

[a] With respect to metallic iron.

caused by the non-uniform distribution of the other transition metals or their lower oxides. The relative amount of iron present in the three different configurations is also given in Table 4. In the fourth stage, α-Fe_2O_3 is partially reduced to metallic iron.

The Mössbauer spectrum of the final product of the dynamic TG of G (Fig. 8, Table 4) consists of a hyperfine spectrum in addition to two quadrupole split spectra. The hyperfine spectrum is characteristic of metallic Fe. Even if iron were to form a solid solution with the other metals such as Cu, Ni and Co, the Mössbauer parameters will not vary much because the concentrations of these metals are very low in the nodules. This sample also shows a quadrupole spectrum which is consistent with a non-uniform distribution of electric fields. The percentage of iron ions in this configuration is calculated to be quite small. In accordance with the earlier assumption that by this stage the iron present in the sample has reduced to metallic form, it is observed that the isomer-shift values of both the quadrupole split spectra are indicative of a Fe^0 charge state. The narrow line widths observed are only an artefact due to very small amounts of iron present in this state. A better computer fit of the complex Mössbauer spectra could have been obtained if it were not for the limitation on the symmetric quadrupoles imposed by the program.

Isothermal thermogravimetric measurements were made of the decomposition of marine manganese nodules in H_2 at 300, 315 and 325 °C and for their reduction in hydrogen at temperatures between 400 and 500 °C. The plot of the fraction reacted (α) versus time (t) is given in Fig. 9 and they are

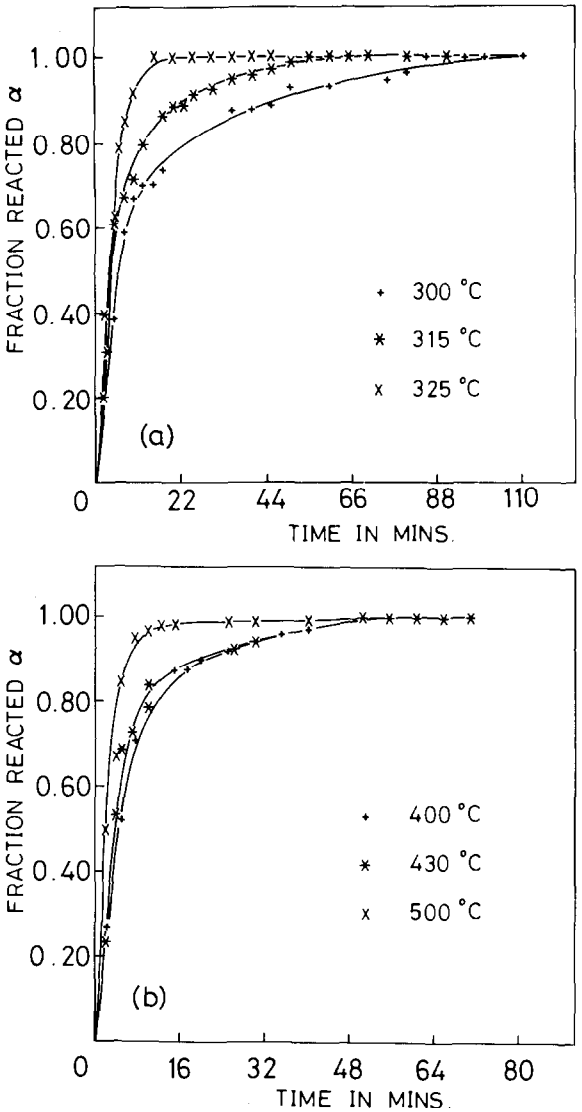

Fig. 9. Plot of fraction reacted (α) versus time (t) for (a) the decomposition reaction, and (b) the reduction reaction.

deceleratory. Activation energies were calculated for the decomposition of manganese nodules and for the reduction of higher oxidation states to lower states in the case of G.

The decomposition reaction is of simple second order and the equation used to obtain the Arrhenius plots is

$$\frac{d\alpha}{dt} = \alpha(1 - \alpha)$$

The Arrhenius plots for the decomposition of oxyhydroxides and for the reduction of the manganese nodules are given in Fig. 10. The activation energies calculated are given in Table 5.

During the decomposition of manganese nodules, the oxyhydroxides are converted to oxides, e.g. the decomposition of ferric oxyhydroxide to α-Fe_2O_3. Due to the presence of hydrogen some of these could be in their lower oxidation states. For the decomposition of nodules and for the reduction of higher oxidation states to lower ones, the activation energy is

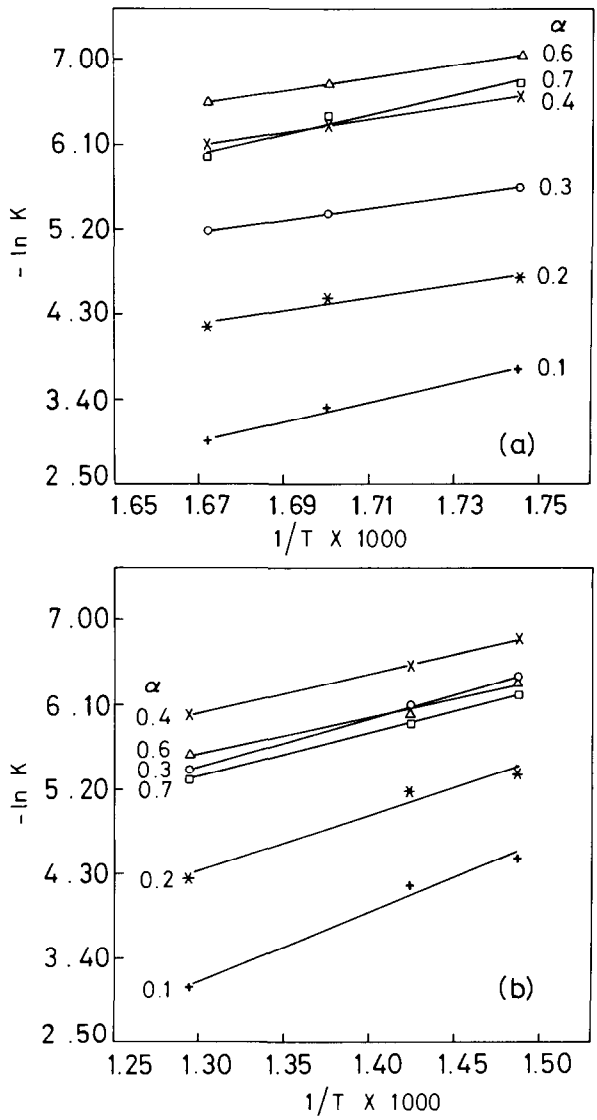

Fig. 10. Arrhenius plots for (a) the decomposition of oxyhydroxides, and (b) the reduction of the manganese nodules.

TABLE 5

Activation energies for the decomposition and reduction of manganese nodules

Fraction reacted (α)	Activation energies [a] (kcal mol^{-1})	
	Decomposition	Reduction
0.1	18.8	
0.2	13.6	14.7
0.3	12.8	11.8
0.4	13.8	10.3
0.6	17.2	8.2
0.7	20.7	7.8
0.8	31.1	9.2

[a] Calculation error = ± 1.

initially high and this may correspond to the nucleation of the product phase. In the case of the decomposition of manganese nodules, there is a progressive increase in the activation energy as α increases from 0.3 to 0.8. This may be due to the outer porous layers offering resistance to the escape of water vapour. The increase in activation energy could also be due to the presence of water vapour on the outer region of each particle resisting the flow of H_2 to the reaction interface or retarding the dehydration reaction between the hydrogen and unreduced manganese nodules at the reaction interface.

In the second case, there is a decrease in the activation energy as α increases from 0.2 to 0.8. This may be due to the reduction of the oxides of Cu, Ni and Co. Metallic Cu obtained first can aid the reduction of nickel oxide to metallic Ni. Both these metals can also influence the reduction of the Co oxide and of α-Fe_2O_3 to metallic form or, alternatively, alloys of Fe with the other metals may be formed [12]. The metallic states of the various elements as and when formed decreases the activation energies. Hence there is a progressive decrease in the activation energy as α increases for the reduction process. The oxides of Cu, Ni, Co, Fe, such as CuO, NiO, Co_3O_4, Fe_2O_3, have their initial reduction temperature, T_i, in hydrogen in the range 200–400 °C and oxides such as Cr_2O_3, Al_2O_3, SiO_2, TiO_2 are not reduced under the same conditions up to 800 °C [13]. These oxides do not exist as pure oxides, but in mixed forms which have higher reduction temperatures. They were not revealed in the present studies as they are present in very dilute concentrations, except for Mn, Fe and SiO_2. Some of these aspects could be clarified by additional Mössbauer measurements as a function of temperature and electron-diffraction studies.

CONCLUSIONS

The reaction of manganese nodules with hydrogen proceeds in four stages. Up to 130 °C there is only loss of water. Up to 320 °C (second stage),

decomposition of ferric oxyhydroxide occurs in addition to other reactions. In the second and third stages there is the possibility of oxides and hydroxides of Cu, Ni and Co being reduced to the metallic state. However, the present experiments do not establish these reactions conclusively. In the fourth stage, there is reduction of α-Fe_2O_3 to metallic Fe or its alloy as confirmed by the Mössbauer studies.

The activation energies for the decomposition of manganese nodules increases with an increase in α from 0.2 to 0.8. This could be due to oxyhydroxides of Fe and Mn decomposing to lower oxides. The activation energies for the reduction of manganese nodules decreases with increasing α. This could be due to the various metal ions formed during the reaction aiding the reduction.

ACKNOWLEDGMENTS

The authors thank Dr. Kurien Jacob for supplying the manganese nodules used in the present work and the Indian Bureau of Mines, Bangalore for their assistance in mineralogical studies on manganese nodules.

REFERENCES

1 R.G. Burns and V.M. Burns, in G.P. Glassby (Ed.), Marine Manganese Deposits, Chap. 7, Elsevier Oceanographic Series, 15 (1977) 185.
2 C. Dodet, F. Noville, M. Crine and J.P. Pirad, Ann. Chim. (Paris), 10 (1985) 7.
3 A.R. Vasudevamurthy, D.S. Bharadwaj and R.M. Mallya, Chem. Ind., (1956) 300.
4 Ramani, M.P. Sathyavathiamma, N.G. Puttaswamy and R.M. Mallya, Mat. Chem. Phys., 9 (1983) 539.
5 A. Okada, T. Okada and Makoto Shima, Sci. Pap. I.P.C.R., (1972) 178.
6 J.S. Stevenson and L.S. Stevenson, Can. Mineral., 10 (1970) 599.
7 G. Constabaris and R.H. Lindquist, Appl. Phys. Lett., 7 (1965) 59.
8 G. Constabaris and R.H. Lindquist, Phys. Rev., 142 (1966) 327.
9 T. Nakumara, T. Shinjo, Y. Endoh, N. Yamamoto, M. Shiga and Y. Nakumara, Phys. Lett., 12 (1984) 178.
10 F. Galembeck, N.F. Leite, L.C.M. Miranda, H.R. Rechenberg and H. Vargo, Phys. Stat. Sol., 60 (1980) 63.
11 D.G. Ramcourt, S.R. Julian and J.M. Daniels, J. Mag. Mag. Mat., 49 (1985) 305.
12 D.N. Drakshayani and R.M. Mallya, unpublished.
13 M. Shimokawabe, R. Furuichi and T. Ishii, Thermochim. Acta, 28 (1979) 287.